Impact-ionization field-effect-transistor based biosensors for ultra-sensitive detection of biomolecules

Deblina Sarkar,[1,a)] Harald Gossner,[2] Walter Hansch,[3] and Kaustav Banerjee[1,a)]
[1]*Department of Electrical and Computer Engineering, University of California, Santa Barbara, California 93106, USA*
[2]*Intel Mobile Communications, Am Campeon 1, 85579 Neubiberg, Germany*
[3]*Institute of Physics, Universität der Bundeswehr München, 85577 Neubiberg, Germany*

(Received 11 March 2013; accepted 21 April 2013; published online 21 May 2013)

The phenomenon of impact-ionization is proposed to be leveraged for a novel biosensor design scheme for highly efficient electrical detection of biological species. Apart from self-consistent numerical simulations, an analytical formalism is also presented to provide physical insight into the working mechanism and performance of the proposed sensor. It is shown that using the impact-ionization field-effect-transistor (IFET) based biosensor, it is possible to obtain an increase in sensitivity of around 4 orders of magnitude at low biomolecule concentration and around 6 orders of magnitude at high biomolecule concentration compared to that in conventional FET (CFET) biosensors. Moreover, IFET biosensors can lead to significant reduction (around 2 orders of magnitude) in response time compared to CFET biosensors. © *2013 AIP Publishing LLC*.
[http://dx.doi.org/10.1063/1.4804577]

Biosensors are indispensable for modern society due to their wide applications in public healthcare, national and homeland security, forensic industries, and environmental protection. Currently, enzyme-linked immunosorbent assay (ELISA) based on optical sensing technology is widely used as a medical diagnostic tool as well as a quality-control check in various industries. For ELISA the labeling of biomolecules is needed, which requires the use of bulky, expensive optical instruments and hence is not suitable for fast point of care clinical applications. On the other hand, the biosensors based on field-effect-transistors (FETs)[1–4] are highly attractive as they promise real-time label-free electrical detection, scalability, inexpensive mass production, and possibility of on-chip integration of both sensor and measurement systems. In a FET biosensor the function of the gate is carried out by the charged biomolecules that are captured by the specific receptors with which the gate dielectric is functionalized. However, there exists fundamental limitations on the sensitivity and response time of conventional FET (CFET) based biosensors.[5–7] Here, we show that the phenomenon of impact-ionization[8–10] can be leveraged to beat these limits, thereby leading to an ultra-sensitive and fast electrical biosensor.

The structure of the proposed nanowire based impact-ionization FET (IFET) biosensor for detecting positively charged biomolecules is shown in Fig. 1. The ends of the nanowire are doped to form a P^+-I-N^+ diode, which is to be operated in the reversed bias mode. Portion of the I-region towards P^+ source is covered with thick oxide to prevent the influence of biomolecules in that region, and we call it the protected region (PR). This region is needed due to the requirement of a threshold length for impact ionization to occur as well as to prevent band-to-band tunneling from valence band of source to conduction band of I-region. The rest of the I-region is covered with a thin oxide for effective *gating effect* through charged biomolecules, and we call it the sensing region (SR).

If the source is biased at a negative voltage such that the reverse bias is below the avalanche breakdown voltage, no impact ionization occurs before biomolecule conjugation (Fig. 2(a)). The attachment of charged biomolecules in SR increases the effective electric field in PR activating impact ionization (Fig. 2(b)). Occurrence of impact ionization leads to a sharp increase in current or, in other words, to ultra-low Subthreshold Swing (*SS*) as shown in Fig. 3. By altering the source voltage this sharp increase in current can be made to occur at very small values of surface potential in SR developed due to biomolecule conjugation (Fig. 3).

While accurate results can be obtained through numerical simulations using Technology Computer Aided Design (TCAD) tools, analytical formalism is necessary for gaining

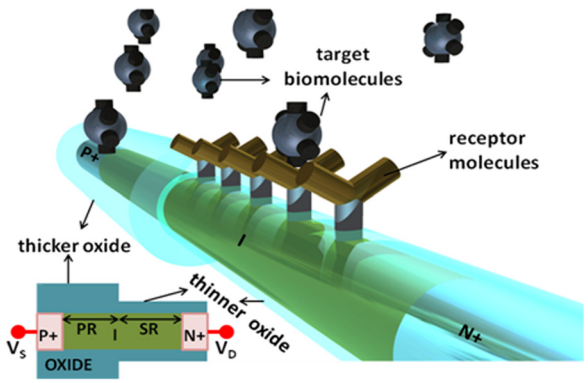

FIG. 1. Schematic diagram of a nanowire based IFET biosensor for detection of positively charged biomolecules. A nanowire structure is chosen to provide high electrostatic control and large surface-to-volume ratio. The inset figure shows the source/drain and channel doping scheme, the PR, and SR in the channel. For detection of negatively charged biomolecules, the position of PR and SR should be interchanged.

[a)]Authors to whom correspondence should be addressed. Electronic addresses: deblina@ece.ucsb.edu and kaustav@ece.ucsb.edu.

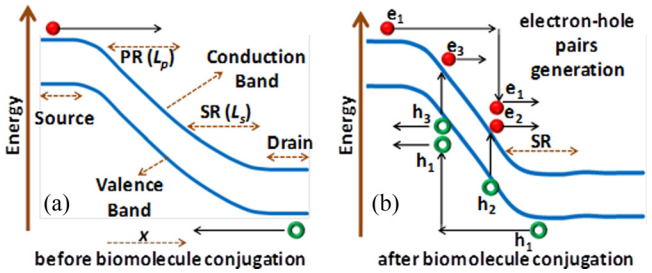

FIG. 2. Band diagram (a) before and (b) after biomolecule conjugation in IFET biosensor. The source is biased at a negative voltage, slightly below the breakdown voltage. Hence, no impact ionization occurs before biomolecule conjugation. Attachment of the biomolecules in the SR leads to increase in electric field in PR (b). Now an electron $\mathbf{e_1}$ can gain enough energy from the electric field to knock out an electron from the valence band creating an electron ($\mathbf{e_2}$) and hole ($\mathbf{h_2}$). Similarly, a hole $\mathbf{h_1}$ can lead to generation of an electron ($\mathbf{e_3}$) and hole ($\mathbf{h_3}$). Thus carriers get multiplied leading to impact ionization.

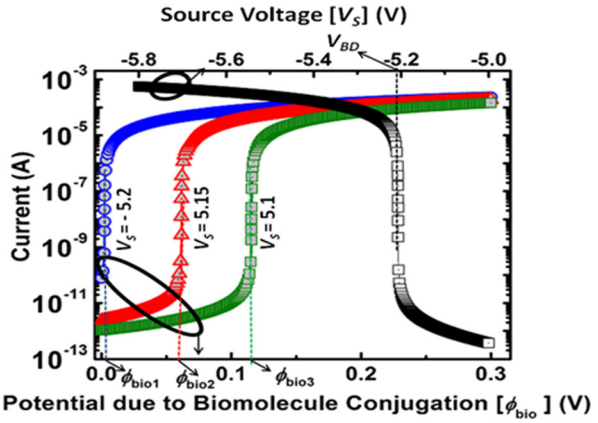

FIG. 3. The black curve (involving left and top axis) shows the current as a function of source voltage (V_s) before biomolecule conjugation. Breakdown occurs when absolute value of V_s is little higher than 5.2 V (marked as V_{BD} in the top axis) leading to sharp increase in current. If the V_s is kept $\leq$5.2 V, the breakdown can be made to occur through the surface potential on the oxide developed due to biomolecule conjugation (ϕ_{bio}) as shown by the blue, red, and green curves (involving left and bottom axis). The values of ϕ_{bio} at which the breakdown occurs depend on the applied V_s and are shown in the figure as ϕ_{bio1}, ϕ_{bio2}, and ϕ_{bio3} for V_s equal to 5.2 V, 5.15 V, and 5.1 V, respectively. It is clear that ϕ_{bio} required for breakdown decreases as source is biased closer to the breakdown point.

easy physical insight. Hence, in the following discussion we focus on deriving analytical formula for sensitivity using a simplified 1D model. The modified 1D Poisson equation for the PR and SR can be written as

$$\frac{d^2\psi_p(x)}{dx^2} = 0, \tag{1a}$$

$$\frac{d^2\psi_s(x)}{dx^2} - \frac{\psi_s(x)+\phi}{\lambda^2} = 0, \tag{1b}$$

respectively. Here, ψ_p and ψ_s are the potential at the semiconductor-oxide interface in PR and SR, respectively, ϕ is the potential at the oxide-electrolyte interface in the SR, x is the direction from source to drain as shown in Fig. 2(a) and is taken to be 0 at the source-PR junction. λ is defined as the natural length scale.[11] The band-bending in the source/drain regions are neglected, which is a valid assumption for highly doped regions. The semiconductor-oxide interface potential at the drain-SR junction is taken as the reference point and hence set to 0, and that at the source-PR junction is defined as U_{src}. Thus, $\psi_s(L_p+L_s)=0$ and $\psi_p(0)=U_{src}$, where L_p and L_s are the lengths of the PR and SR, respectively, as shown in Fig. 2(a). The other two boundary conditions for solving the Poisson equations given by Eq. (1) are obtained from the continuity equations between ψ_p and ψ_s and their derivatives as $\psi_p(L_p)=\psi_s(L_p)$ and $d\psi_p(x)/dx|_{x=L_p} = d\psi_s(x)/dx|_{x=L_p}$. The solution of the potentials is given by

$$\psi_p(x) = -\frac{\{(U_{src}+\phi)\cosh(L_s/\lambda)-\phi\}x}{\lambda\sinh(L_s/\lambda)+L_p\cosh(L_s/\lambda)} + U_{src}, \tag{2a}$$

$$\psi_s(x) = \frac{\lambda(U_{src}-\phi)\sinh((L_p+L_s-x)/\lambda)+L_p\phi\cosh((x-L_p)/\lambda)}{\lambda\sinh(L_s/\lambda)+L_p\cosh(L_s/\lambda)} + \frac{\lambda\phi L_p\phi\sinh((x-L_p)/\lambda)}{\lambda\sinh(L_s/\lambda)+L_p\cosh(L_s/\lambda)} - \phi. \tag{2b}$$

Since impact ionization occurs in the PR, it is necessary to simplify the equation of semiconductor-oxide interface potential in that region given by Eq. (2a) in order to obtain simplified equation for the impact ionization current. It is to be noted that the impact of SR has been intrinsically incorporated in Eq. (2a) through the factors ϕ, λ, and L_s. Using the condition $L_s \gg \lambda$, which is the case in an electrostatically well controlled device, Eq. (2a) can be simplified as

$$\psi_p(x) = -\frac{(U_{src}+\phi)\,x}{\lambda+L_p} + U_{src}. \tag{3}$$

Using Eq. (3), the electric field in the PR can be derived as

$$F_p = \frac{(U_{src}+\phi)}{\lambda+L_p}. \tag{4}$$

This electric field can be used to calculate the impact ionization coefficient α, which is defined as the number of electron-hole pairs generated by a carrier per unit distance travelled and is given by $\alpha = \alpha_\infty e^{-F_{crit}/|F_p|}$, where α_∞ is an empirical parameter and F_{crit} is the critical electric field. For deriving a simplified analytical solution, α_∞ and F_{crit} for electrons and holes are assumed to be similar,[12] and thus the ionization integral M can be written as $M = \int_0^{L_p} \alpha\, dx$. Using Eq. (4) M can be derived as

$$M = L_p\,\alpha_\infty e^{-F_{crit}/\left|\frac{(U_{src}+\phi)}{\lambda+L_p}\right|}. \tag{5}$$

The avalanche breakdown occurs when M reaches the value of 1. Now, the potential ϕ can be divided into two parts: the initial potential ϕ_0 which can be adjusted using the electrolyte reference electrode and the potential developed due to biomolecule conjugation ϕ_{bio}. The threshold value of the potential due to biomolecule attachment that is required for avalanche breakdown (ϕ_{bio_th}) can be derived by equating M to 1, and thus we obtain

$$\phi_{bio\_th} = \frac{F_{crit}(\lambda + L_p)}{\ln(\alpha L_p)} - U_{src} - \phi_0. \tag{6}$$

For $\phi_{bio} < \phi_{bio\_th}$, the current ($I_i$) is given by $I_{rev}/(1\text{-}M)$ where I_{rev} is the reverse biased P-I-N junction current. Thus we can write

$$I_i = I_{rev} \Big/ \left\{1 - L_p\,\alpha_\infty e^{-F_{crit}/\left|\frac{(U_{src}+\phi_0+\phi_{bio})}{\lambda+L_p}\right|}\right\} \quad for\ \phi_{bio} < \phi_{bio\_th}. \tag{7}$$

After avalanche breakdown the current in the IFET biosensor will behave like the conventional FET with an effective drain-to-source voltage (V_{ds_eff}) equal to the potential at $x = L_p$ at $\phi_{bio} = \phi_{bio\_th}$. Using Eqs. (3) and (6), V_{ds_eff} can be derived as

$$V_{ds\_eff} = -\frac{F_{crit}\,L_p}{\ln(\alpha L_p)} + U_{src}. \tag{8}$$

Now, the current (I_c) for $\phi_{bio} > \phi_{bio\_th}$ can be written as

$$I_c = \mu W/(2L_s)\ C\{\phi - (\phi_0 + \phi_{bio\_th})\}^2 \quad for\ \phi_{bio} - \phi_{bio\_th} < V_{ds\_eff}, \tag{9a}$$

$$I_c = \mu W/L_s C\{(\phi - (\phi_0 + \phi_{bio\_th}))V_{ds\_eff} - {V_{ds\_eff}}^2/2\} \quad for\ \phi_{bio} - \phi_{bio\_th} > V_{ds\_eff}. \tag{9b}$$

Here W is the width of the device and C is the gate dielectric capacitance. Using the equations of current given by Eqs. (7) and (9), analytical formulae for sensitivity can be derived where sensitivity is defined as the ratio of the change in current due to biomolecule conjugation to the initial current before conjugation. For $\phi_{bio} < \phi_{bio\_th}$, S_n is derived as

$$S_n = \left\{1 - L_p\,\alpha_\infty e^{-F_{crit}/\left|\frac{(U_{src}+\phi_0)}{\lambda+L_p}\right|}\right\} \Big/ \left\{1 - L_p\,\alpha_\infty e^{-F_{crit}/\left|\frac{(U_{src}+\phi_0+\phi_{bio})}{\lambda+L_p}\right|}\right\} - 1. \tag{10a}$$

For $\phi_{bio} > \phi_{bio\_th}$, S_n can be written as

$$S_n = \frac{I_c - I_i}{I_i}. \tag{10b}$$

From the analytical derivations it can be observed that the sensitivity is dependent on the initial condition of the IFET, which can be tuned by source and reference gate bias, thus modulating U_{src} and ϕ_0, respectively. These two knobs should be adjusted in such a way that the IFET biosensor is always below the breakdown potential before biomolecule conjugation. Also, it is clear from Eq. (6) that by proper tuning of U_{src} and ϕ_0, the threshold value of potential due to biomolecule conjugation can be reduced, and thus a fewer number of biomolecules attaching to the biosensor surface will be able to cause a substantial increase in the current.

Fig. 4(a) shows the results of source bias sweep calculated through TCAD simulations in IFET biosensor before and after the biomolecule conjugation for different values of biomolecule concentration (ρ_0) in the electrolyte. The results of drain voltage sweep for a CFET biosensor is shown in Fig. 4(b). Because of the sharp increase in current due to impact ionization in IFET, the current curves after biomolecule conjugation are distinctly distinguishable from the one before the conjugation even at very small values of ρ_0. For CFET biosensors, on the other hand, there is very small change in current after conjugation as ρ_0 is decreased. In Fig. 5(a), the sensitivity is plotted as a function of ρ_0 for CFET and two different bias points of IFET. When V_s and ϕ_0 in IFET are adjusted to obtain the minimum SS (bias pt1), even low ρ_0 can lead to sharp increase in current and hence very high sensitivity (around 4 orders of magnitude higher compared to CFET). However, if IFET is biased at lower V_s (bias pt2) high ρ_0 is required in order for breakdown to occur. Once sufficient ρ_0 is reached, current and hence sensitivity increases sharply. For higher values of ρ_0, sensitivity at bias pt2 is higher (around 6 orders of magnitude higher compared to CFET) than that at bias pt1 (around 2.5 orders of magnitude higher compared to CFET) because of the lower initial current before biomolecule conjugation at bias

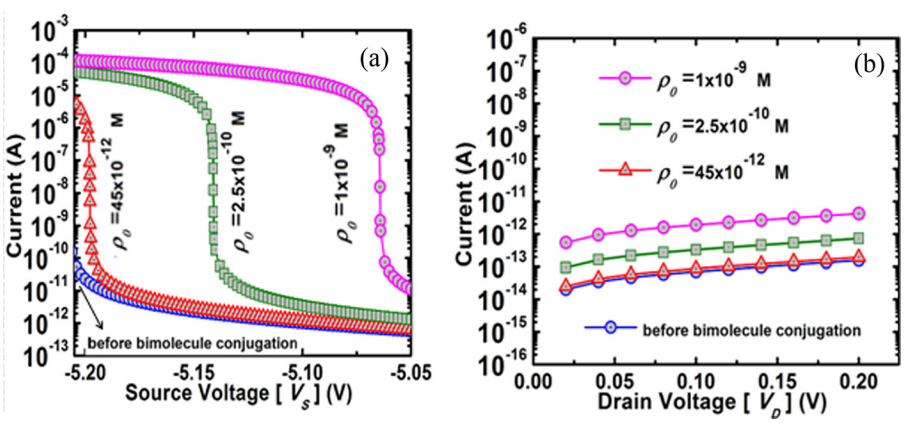

FIG. 4. The current as a function of source bias in (a) IFET and (b) CFET biosensor before and after biomolecule conjugation for different values of biomolecule concentration (ρ_0) in the electrolyte. Unless mentioned otherwise, all simulations in this paper are done for a silicon nanowire with diameter of 30 nm with enclosing oxide thickness of 3 nm in the sensing region, and the ionic concentration I_0 is taken as 10^{-5} M.

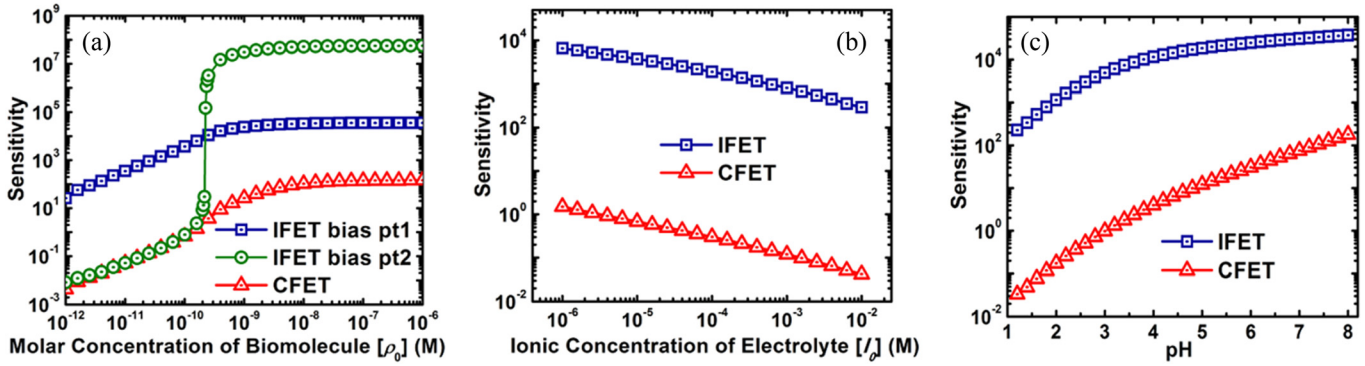

FIG. 5. (a) Sensitivity of both IFET and CFET biosensors as a function of biomolecule concentration (ρ_0). Bias pt1 refers to the condition of IFET where V_s and ϕ_0 are adjusted to obtain the minimum *SS* while bias pt2 refers to the condition when V_s is 0.05 V below that in bias pt1. The average SS of the IFET over 3 orders of magnitude of drain current is around 1.7 mV/dec. (b) Sensitivity as a function of ionic concentration (I_0). While sensitivity decreases for both IFET and CFET biosensors with the increase in I_0 due to electrostatic screening, the IFET biosensor still exhibits substantially higher sensitivity. (c) Sensitivity comparison between IFET and CFET biosensors for pH sensing as a function of pH values. For (b) and (c) IFET is at bias pt 1.

pt1. Since high sensitivity at low biomolecule concentration is desirable, bias pt1 is preferable for IFET biosensor operation. As is clear from Fig. 5(b), advantage of IFET biosensor over CFET is retained even when the ionic concentration of the electrolyte is increased (which increases the electrostatic screening by the ions). Fig. 5(c) shows the sensitivity comparison between IFET and CFET biosensors for pH sensing. The pH sensing is based on the change in surface charge due to protonation/deprotonation of the OH groups on the enclosing oxide surface, which depends on the concentration of H^+ ions and hence on the pH value. It is observed that IFET biosensor can lead to around 4 orders of magnitude increase in sensitivity compared to that in CFET for pH detection.

Apart from sensitivity, another critical parameter for gauging the performance of the biosensors is the response time. Response time (t_r) is defined as the time required to obtain a desired sensitivity. Before a target analyte molecule can bind at the sensor surface and electrostatically modulate the channel conductance, the molecule must diffuse from the bulk solution to the sensor surface. This diffusion process takes time and sets lower limits on achievable detection times at a given analyte concentration.[13] Hence, a more specific definition of response time is the time needed to capture a certain surface density of biomolecules (N_{bio})[14] in order to achieve a desired change in electrical signal. Fig. 6(a) illustrates that t_r is directly proportional to the required N_{bio} and inversely proportional to ρ_0. Fig. 6(b) shows that the IFET can lead to significant reduction in response time compared to CFET. This effect can be understood in the following way. Extremely low *SS* of IFET implies that for obtaining the same change in current and hence same sensitvity, the required change in surface potential (ϕ_{bio}) is much lower in IFET compared to that in CFET. Since t_r is directly proportional to N_{bio}, which is again directly proportional to ϕ_{bio}, decrease in ϕ_{bio} leads to decrease in N_{bio} and consequently to reduction in t_r. From Fig. 6(b) we can also conclude that within a same desired response time, IFET can detect biomolecules at substantially lower biomolecule concentrations.

It is to be noted that tunnel-FETs (TFETs) employing interband tunneling[15] can also lead to sharper increase in current or lower *SS* compared to CFETs and hence is attractive as a sensor for biomolecules[5,6] as well as gaseous species.[16] The best reported *SS* value for TFETs is 30 mV/dec,[17,18] and further improvement is expected. The phenomenon of impact ionization has been shown to lead to *SS* as low as 72 μV/decade.[19] The IFETs based on silicon, however, have very high breakdown voltage, and application of strain or alternate materials/design is required for lowering the operating bias.[10,20] Hence, from an ultra-low power

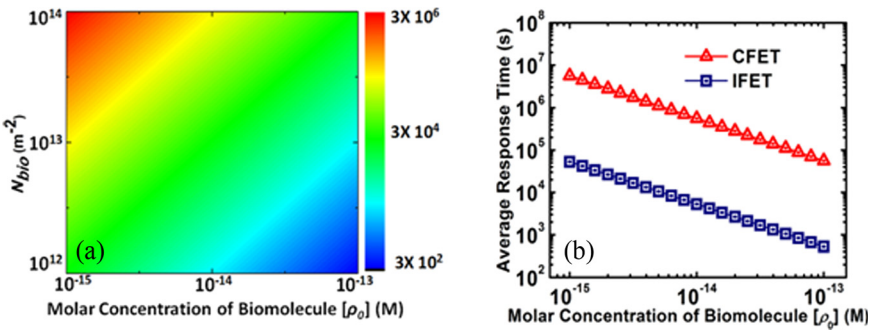

FIG. 6. (a) The colormap showing the average response time (t_r) in seconds of the biosensor as a function of the required surface density of biomolecules (N_{bio}) on the oxide surface to achieve the desired sensitivity, and the concentration (ρ_0) of the biomolecules in the solution. t_r increases as ρ_0 is decreased as it takes more time to capture the biomolecules when its concentration in the solution is low. t_r increases with increase in N_{bio}. This is because if the required surface density of biomolecules is more, it will take more time to reach that value. (b) Average response time as a function of the biomolecule concentration (ρ_0). For the same value of ρ_0, IFET can lead to significant reduction in t_r. If the response time is kept constant, then within the same desired t_r, IFET can lead to detection at much lower biomolecule concentrations.

perspective, the TFET biosensors remain attractive. Reliability of IFETs can be improved using novel vertical structures[9] thus making reusability of the IFET biosensor feasible. Although in this paper the results are presented for silicon nanowire based IFETs, the general discussion is valid for other materials and structures as well.

In summary, an impact-ionization based biosensor is proposed, and it is shown that it can lead to substantial increase in sensitivity and decrease in response time compared to CFET biosensors. Thus, IFET biosensors can be extremely promising for applications where ultra-high sensitivity and fast response is desirable such as for early detection of deadly diseases or prevention against biological accidents or attacks.

This work was supported in part by the U.S. National Science Foundation, Grant No. CCF-1162633. K.B. would also like to thank the Alexander von Humboldt Foundation in Germany for facilitating this collaboration through the F.W. Bessel Research Award.

[1]E. Souteyrand, J. P. Cloarec, J. R. Martin, C. Wilson, I. Lawrence, S. Mikkelsen, and M. F. Lawrence, J. Phys. Chem. B **101**, 2980 (1997).
[2]J. Fritz, E. B. Cooper, S. Gaudet, P. K. Sorger, and S. R. Manalis, Proc. Natl. Acad. Sci. U.S.A. **99**, 14142 (2002).
[3]Y. Cui, Q. Wei, H. Park, and C. M. Lieber, Science **293**, 1289 (2001).
[4]M. W. Shinwari, M. J. Deen, and D. Landheer, Microelectron. Reliab. **47**, 2025 (2007).
[5]D. Sarkar and K. Banerjee, Appl. Phys. Lett. **100**, 143108 (2012).
[6]D. Sarkar and K. Banerjee, in *Proceedings of the Device Research Conference* (IEEE, 2012), p. 83.
[7]A. Moscatelli, P. Rodgers, M. Segal, and O. Vaughan, "Biomolecular turn-ons," Nat. Nanotechnol. **7**, 275 (2012).
[8]K. Gopalakrishnan, P. B. Griffin, and J. D. Plummer, IEDM Tech. Dig. **2002**, 289.
[9]U. Abelein, A. Assmuth, P. Iskra, M. Schindler, T. Sulima, and I. Eisele, Solid-State Electron. **51**, 1405 (2007).
[10]D. Sarkar, N. Singh, and K. Banerjee, IEEE Electron Devices Lett. **31**, 1175 (2010).
[11]R.-H. Yan, A. Ourmazd, and K. F. Lee, IEEE Trans. Electron Devices **39**, 1704 (1992).
[12]U. Mishra, *Semiconductor Device Physics and Design* (Springer, Dordrecht, The Netherlands, 2008).
[13]P. E. Sheehan and L. J. Whitman, Nano Lett. **5**, 803 (2005).
[14]P. R. Nair and M. A. Alam, Appl. Phys. Lett. **88**, 233120 (2006).
[15]D. Sarkar, M. Krall, and K. Banerjee, Appl. Phys. Lett. **97**, 263109 (2010).
[16]D. Sarkar, H. Gossner, W. Hansch, and K. Banerjee, Appl. Phys. Lett. **102**, 023110 (2013).
[17]R. Gandhi, Z. Chen, N. Singh, K. Banerjee, and S. Lee, IEEE Electron Devices Lett. **32**, 437 (2011).
[18]R. Gandhi, Z. Chen, N. Singh, K. Banerjee, and S. Lee, IEEE Electron Devices Lett. **32**, 1504 (2011).
[19]Z. Lu, N. Collaert, M. Aoulaiche, B. De Wachter, A. De Keersgieter, J. G. Fossum, L. Altimime, and M. Jurczak, in *IEEE Int. Electron Devices Meeting (IEDM)* (IEEE, 2010), pp. 16.6.1–16.6.3.
[20]W. Y. Choi, J. Y. Song, J. P. Kim, S. W. Kim, J. D. Lee, and B.-G. Park, in Proceedings of Nanotechnology Device Material Conference, 2006, p. 380.